Nitrogen mineralization and immobilization in sediments of the East China Sea: Spatiotemporal variations and…

Article *in* Journal of Geophysical Research: Biogeosciences · November 2016

DOI: 10.1002/2016JG003499

CITATION
1

READS
97

8 authors, including:

Lijun Hou
East China Normal University
98 PUBLICATIONS **1,323** CITATIONS
SEE PROFILE

Xiaofei Li
East China Normal University
33 PUBLICATIONS **162** CITATIONS
SEE PROFILE

Yanling Zheng
East China Normal University
28 PUBLICATIONS **234** CITATIONS
SEE PROFILE

Juan Gao
East China Normal University
17 PUBLICATIONS **71** CITATIONS
SEE PROFILE

AGU PUBLICATIONS

JGR

Journal of Geophysical Research: Biogeosciences

RESEARCH ARTICLE
10.1002/2016JG003499

Xianbiao Lin and Lijun Hou contributed equally to this work.

Key Points:
- Sediment N mineralization and immobilization in the East China Sea were examined with N isotope dilution technique
- N mineralization and immobilization are associated tightly with sediment physicochemical characteristics
- Sediment N mineralization and immobilization play an important role in controlling the N budget in the coastal marine ecosystem

Supporting Information:
- Supporting Information S1

Correspondence to:
L. Hou,
ljhou@sklec.ecnu.edu.cn

Citation:
Lin, X., L. Hou, M. Liu, X. Li, Y. Zheng, G. Yin, J. Gao, and X. Jiang (2016), Nitrogen mineralization and immobilization in sediments of the East China Sea: Spatiotemporal variations and environmental implications, *J. Geophys. Res. Biogeosci.*, *121*, 2842–2855, doi:10.1002/2016JG003499.

Received 22 MAY 2016
Accepted 27 OCT 2016
Accepted article online 29 OCT 2016
Published online 18 NOV 2016

Nitrogen mineralization and immobilization in sediments of the East China Sea: Spatiotemporal variations and environmental implications

Xianbiao Lin[1], Lijun Hou[2], Min Liu[1], Xiaofei Li[1], Yanling Zheng[1], Guoyu Yin[1], Juan Gao[2], and Xiaofen Jiang[2]

[1]College of Geographical Sciences, East China Normal University, Shanghai, China, [2]State Key Laboratory of Estuarine and Coastal Research, East China Normal University, Shanghai, China

Abstract Nitrogen (N) mineralization and immobilization are important processes of N biogeochemical cycle in marine sediments. This study investigated gross N mineralization (GNM) and NH_4^+ immobilization (GAI) in the sediments from the East China Sea (ESC), using ^{15}N stable isotope dilution technique. Results show that measured rates of GNM and GAI ranged from 0.04 to 6.1 $\mu g\,N\,g^{-1}\,d^{-1}$ and from undetectable to 9.82 $\mu g\,N\,g^{-1}\,d^{-1}$, respectively. In general, both GNM and GAI rates were significantly greater in summer as compared to winter, and the high rates occurred mainly in the muddy area and increased gradually from the Yangtze Estuary to Zhe-Min Coastal muddy areas. The GNM and GAI processes were related closely to sediment temperature, pH, ammonium (NH_4^+), nitrate (NO_3^-), total organic carbon (TOC), and total nitrogen (TN) contents in the muddy area, while they were associated tightly with sediment temperature, pH, NH_4^+, TOC, TN, sulfide, and Fe(III) concentrations in the sandy area. In addition, the total mineralized and immobilized N in the East China Sea (ECS) were estimated to be approximately 2.1×10^6 t N yr^{-1} and 2.7×10^6 t N yr^{-1}, respectively. Overall, these results highlight the importance of N mineralization and immobilization in controlling the N budget in the ECS and improve the understanding of both processes and associated controlling mechanisms in the coastal marine ecosystem.

1. Introduction

Nitrogen (N) mineralization is an important biogeochemical process that converts N from organic into inorganic forms by heterotrophic microorganisms and serves as a source of energy in microbial metabolisms [*Benbi and Richter*, 2002; *Mishra et al.*, 2005]. This process in sediments also acts as an important internal source of N and makes contribution to eutrophication in organic matter-riched acquatic envoronments [*Benbi and Richter*, 2002; *Matheson et al.*, 2003; *Kalvelage et al.*, 2013; *Li et al.*, 2014]. In contrast, N immobilization is an inversed process that transforms the inorganic N into organic N, including NH_4^+ and NO_3^- immobilization [*Tremblay and Benner*, 2006; *Zhu et al.*, 2013b]. Nevertheless, microbes preferentially assimilate NH_4^+ due to higher energy costs associated with biological NO_3^- assimilation, and thus, the presence of NH_4^+ may greatly inhibit microbial NO_3^- immobilization [*Zhu et al.*, 2013b]. Meanwhile, NO_3^- immobilization plays a negligible role in total microbial N immobilization under anaerobic conditions [*Zhao et al.*, 2015]. Moreover, numerous studies have demonstrated that microbial NH_4^+ immobilization is the dominant process of NH_4^+ consumption [*Di et al.*, 2000; *Bengtsson et al.*, 2003; *Bedard-Haughn et al.*, 2013; *Gütlein et al.*, 2016], which can effectively remove the accumulated NH_4^+ in sediments and maintain ecological health [*Matheson et al.*, 2003]. Coastal marine areas are the transitional zones between land and open sea and play an important role in the N biogeochemical cycle. During the past few decades, N mineralization and/or immobilization have been examined in coastal marine sediments [*Billen*, 1978; *Blackburn*, 1979; *Boynton et al.*, 1980; *Jensen et al.*, 1990; *Hansen and Blackburn*, 1991; *Cufrey and Kemp*, 1992; *Anderson et al.*, 1997; *Caraco et al.*, 1998; *Herbert*, 1999; *Rysgaard et al.*, 2000]. However, most of these studies report net mineralization rates only and that data on immobilization are missing almost completely. Therefore, an improved understanding of N mineralization and immobilization is essential for evaluation of the nutrient balance in coastal marine ecosystems.

The East China Sea (ECS) is the largest marginal sea in northwestern Pacific, which is profoundly influenced by the Yangtze River [*Zhang et al.*, 2015; *Gao et al.*, 2015]. Annually, it receives substantial terrestrial materials, including particulate organic matter (approximately 1.20×10^7 t yr^{-1}) [*Liu et al.*, 2007] and dissolved inorganic

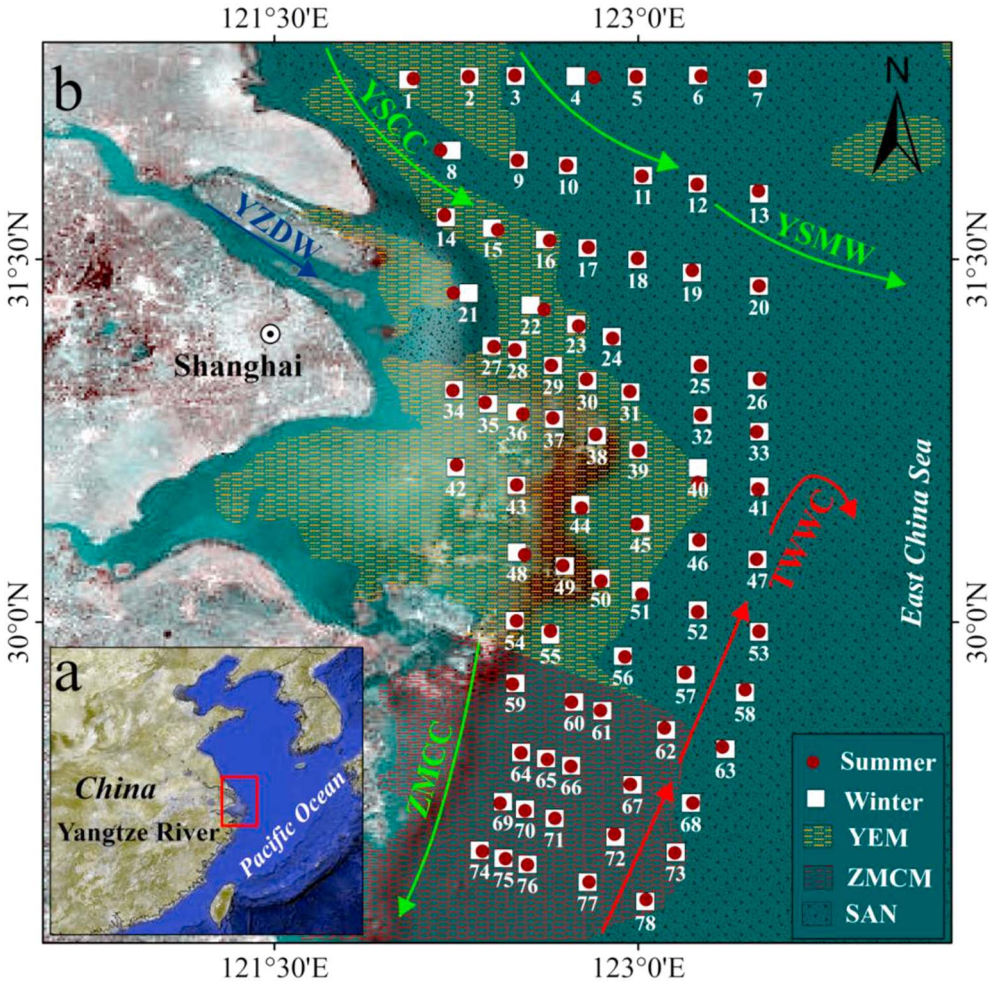

Figure 1. (a and b) Location of the East China Sea (ECS) and sampling sites. The mud-deposits, Yangtze Estuary Mud area (YEM) and Zhe-Min Coastal Mud area (ZMCM), are displayed according to *Qin* [1996]. The arrows indicate the direction of the currents. YZDW: Yangtze River Diluted Water, YSCC: Yellow Sea Coastal Current, YSMW: Yellow Sea Mixing Water, ZMCC: Zhe-Min Coastal Current, TWWC: Taiwan Warm Current. This true-color Moderate Resolution Imaging Spectroradiometer image is obtained from the U.S. Geological Survey EROS Visible Earth website (http://landsatlook.usgs.gov/viewer.html).

nitrogen ($1.2–2.42 \times 10^6$ t N yr^{-1}) [*Huang et al.*, 2006; *Kim et al.*, 2011; *Xu et al.*, 2013; *Chen et al.*, 2016]. In particular, the excessive input of anthropogenic N has caused serious environmental risks such as eutrophication and hypoxia in the ECS during the past several decades [*Li et al.*, 2011; *Cui et al.*, 2013; *Song et al.*, 2013]. Thus, the N biogeochemical processes are of great concern in the ECS. However, most of previous studies have mainly focused on the source, distribution, and deposition of N as well as dissimilatory nitrate reduction processes (including denitrification, dissimilatory nitrate reduction to ammonium, and anaerobic ammonium oxidation) in the ECS [*Chen and Wang*, 1999; *Gao et al.*, 2012; *Hou et al.*, 2013; *Song et al.*, 2013; *Zhu et al.*, 2013a; *Deng et al.*, 2015; *Gao et al.*, 2015]. To date, few studies have examined sedimentary N mineralization and immobilization and their associations with environmental factors [*Lin et al.*, 2016]. Therefore, quantifying the internal N mineralized and immobilized and understanding the pattern of main factors affecting these processes are both critical for the assessment of the N budget and maintenance of the ecological and environmental health in the ECS.

In this study, we used ^{15}N isotope dilution technique to quantify gross N mineralization (GNM) and NH_4^+ immobilization (GAI) rates in sediments of the ECS. Environmental variables were measured to elucidate their correlations with the processes of both N mineralization and immobilization. We also determined the relative NH_4^+ immobilization (RAI) and the percentage of NH_4^+ mineralized (PAM) to reveal the potential implications

of both N mineralization and immobilization for the evalution of the N budget in the coastal margin ecosystem.

2. Materials and Methods

2.1. Study Area

The ECS is the largest marginal sea in the northwestern Pacific and includes an entensive area of shallow continental shelf (approximately 7.7×10^5 km^2), with a mean water depth of approximately 72 m (Figure 1a). The topography gently slants from the continental shelf toward the southeast, with a mean slope of 0.04% [*Zhang et al.*, 2004; *Wu et al.*, 2016]. An approximately 800 km long muddy zone exists along the southern coast of the Yangtze Delta and extends to the northern Taiwan Strait [*Liu et al.*, 2007]. Several intricate currents appear in the ECS (Figure 1b), including the Yangtze River Diluted Water (YZDW), two northward currents (the Taiwan Warm Current and the Kuroshio Current), and two southward currents (the Yellow Sea Coastal Current and the Zhe-Min Coastal Current) [*Liu et al.*, 2010a; *Wu et al.*, 2016]. These currents generally dominate the circulation of the ECS and significantly affect the distributions of both water masses and sedimentation [*Wang et al.*, 2016]. Meanwhile, the ECS is a typical riverine-dominated ocean margin system, which receives approximately 3.97×10^8 t yr^{-1} of terrestrial sediment from the Yangtze River [*Liu et al.*, 2007; *Kim et al.*, 2011; *Yu et al.*, 2012]. Additionally, the Yangtze River annually exports large amounts of nutrients and carbon to the ECS, consequently enhancing the coastal eutrophication and red tides during the past several decades [*Li et al.*, 2011].

2.2. Sample Collection

Sediment samples were collected by using a box corer and subsampled with Plexiglas tubes (7 cm diameter) from 78 sites of the ECS (Figure 1b) in the winter (11 February to 10 March 2014) and summer (10 to 18 July 2014) cruises, respectively. At each site, triplicate sediment cores (0–5 cm deep) were collected, sealed immediately with air-tight and acid-cleaned plastic bags, and stored at 4°C. In the laboratory, sediment in each core was immediately mixed thoroughly under helium (He). One part of the sediment sample was used for the measurement of N mineralization and immobilization rates through sediment-slurry incubation experiments and the other portion for the analysis of sediment physicochemical parameters.

2.3. Determination of Environmental Parameters

Temperature, salinity, and water depth were determined in situ with a conductivity-temperature-depth profiler (Sea-Bird 911 plus). Sediment pH was measured by using a pH meter (Mettler-Toledo), after sediment was thoroughly mixed with CO_2-free deionized water in 1:2.5 volume ratio [*Zheng et al.*, 2014]. Sediment water contents were calculated gravimetrically from fresh sediment dried at 60°C to a constant value [*Hou et al.*, 2013; *Wang et al.*, 2016]. Exchangeable NH_4^+ and NO_3^- in sediments were extracted with 2 M KCl and determined by using a continuous-flow nutrient analyzer (SAN Plus, *Skalar Analytical* B.V., the Netherland) with detection limits of 0.5 and 0.1 μM for NH_4^+ and for NO_3^-, respectively. Organic carbon (total organic carbon (TOC)) and N (total nitrogen (TN)) of sediment were analyzed on an elemental analyzer (VarioEL III) after sediment was acidified to remove inorganic carbon [*Hou et al.*, 2013]. Sediment grain size was measured by using a LS 13320 Laser grain sizer [*Wang et al.*, 2016]. Sulfide in sediments was determined by using a silver-sulfide electrode (Thermo Scientific Orion) with a detection limit of 0.09 μM [*Hou et al.*, 2013]. Ferric oxides in sediments were extracted with a mixture of both 0.5 M HCl and 0.25 M hydroxylamine hydrochloride and analyzed with the ferrozine-based colorimetric method [*Roden and Lovley*, 1993; *Deng et al.*, 2015].

2.4. Sediment-Slurry Incubation Experiments

Considering that sediment generally remains anoxic [*Deng et al.*, 2015; *Zheng et al.*, 2016], rates of GNM and GAI were determined through anaerobic incubations by using ^{15}N isotope dilution technique [*Lin et al.*, 2016]. Briefly, each sediment sample was transferred to a borosilicate container together with filtered site benthic water (in 1:5 volume ratio), homogenized, and flushed by He (30 min), and then the resulting sediment slurry was transferred into six gastight Exetainer vials (12.0 mL, Labco). Vials were preincubated in dark at near in situ temperature for approximately 2–4 h to remove potential ambient O_2. After this preincubation, $^{15}NH_4^+$ solution, which was made with $^{15}NH_4Cl$ (99.09 at. %; Cambridge Isotope Laboratories, Inc., Tewksbury, MA, USA), was injected into the anaerobic vials, with a final concentration of approximately 2 μg ^{15}N g^{-1} and a final $\%^{15}N$ of approximately 5–10% depending on the initial NH_4^+ contents [*Huygens et al.*, 2013]. Half of

the vials were sacrificed immediately with the addition of 100 μL saturated $HgCl_2$, and the remaining slurries were incubated in dark at near in situ temperature for 24 h on a shaker table (150 rpm). After 24 h, these remaining slurries were also injected with $HgCl_2$ to stop the incubation. NH_4^+ was then extracted with 2 M KCl from the initial and final sediment slurries [*Lin et al.*, 2016]. After extraction, the total NH_4^+ (including $^{14}NH_4^+$ and $^{15}NH_4^+$) in extractants was analyzed as described above, while the $^{15}NH_4^+$ in extractants was oxidized with hypobromite iodine to N_2 and determined with membrane inlet mass spectrometer [*Yin et al.*, 2014].

GNM and NH_4^+ consumption rates were quantified as described in *Kirkham and Bartholomew* [1954] by using equations (1) and (2), respectively.

$$m = \frac{M_i - M_f}{t} \times \frac{\log(H_i M_f / H_f M_i)}{\log(M_i / M_f)} \quad (1)$$

$$c = \frac{M_i = M_f}{t} \times \frac{\log(H_i / H_f)}{\log(M_i / M_f)} \quad (2)$$

where m and c (μg N g^{-1} d^{-1}) are the rates of GNM and NH_4^+ consumption, M_i and M_f (μg N g^{-1}) are the respective concentrations of total NH_4^+ in initial and final sediment slurries, H_i and H_f (μg N g^{-1}) are the respective concentrations of $^{15}NH_4^+$ in initial and final sediment slurries, and t (day) is the incubation time. In the assumption NH_4^+ consumption through nitrification and volatilization was negligible under an anaerobic condition [*Di et al.*, 2000], and the GAI rate was equivalent to the gross NH_4^+ consumption rate. Meanwhile, NO_3^- immobilization plays a negligible role in this study, because this process occurs under oxic conditions. Hence, the GAI can represent the N immobilization in our incubation experiments. In addition, the percentage of NH_4^+ mineralized per day (PAM) was referred to as the rates of GNM divided by sediment N contents and multiplied by 100. Relative NH_4^+ immobilization (RAI) is the ratio of GAI to GNM rates.

2.5. Statistical Analyses

All statistical analyses were performed with SPSS 19.0 in this study. Pearson's correlation analysis was performed to determine the correlations between environmental parameters and N transformation rates. One-way analysis of variance (ANOVA), followed by Tukey's honest significant difference test, was also conducted to compare measured rates and physicochemical properties.

3. Results

To better reveal spatial and temporal differences in N mineralization and immobilization, all sampling sites were categorized into three groups: (1) the Yangtze Estuary muddy area (YEM), (2) the Zhe-Min Coastal muddy area (ZMCM), and (3) the sandy area (SAN) (Figure 1b), based on location of sampling sites and grain size composition of sediments (Table S1 in the supporting information).

3.1. Station Characteristics

Environmental characteristics of bottom water and sediments from the ECS are given in Figure 2 and Table S1. The water depth of the sampling sites ranged from 6 to 67 m, and the mean water depth was 37.6 ± 17.1 m (Table S1). Summer temperature of bottom water ranged from 18.6 to 26°C, with a mean value of 21 ± 2.2°C, while winter temperature of bottom water varied from 5.4 to 14.1°C, with a mean value of 9.6 ± 2.6°C (Table S1). The salinity of the bottom water varied from 0.5 to 31.4 in summer and from 26.3 to 33.9 in winter (Table S1). The sediment median grain size (MΦ) varied considerably in summer (5.19–261.10 μm) and winter (6.06–305.70 μm), with the mean values being higher in winter (79.84 ± 88.85 μm) than in summer (71.74 ± 82.91 μm). Thus, the shelf regions of the ECS were characterized by sandy deposits which generally contained more than 50% sand, while sediments deposited in the inner shelf of the ECS were characterized by fine particles with high contents of silt (>55%) and clay (>25%) (Figures 2c and 2d and Table S1). The contents of TOC varied from 0.70 to 9.84 mg g^{-1} in summer and from 0.02 to 8.10 mg g^{-1} in winter, with a marked seasonal difference (one-way ANOVA, $p < 0.001$). The concentrations of TN also had a significantly seasonal change (one-way ANOVA, $p < 0.001$), with values of 0.05–0.99 mg g^{-1} in summer and 0.01–1.09 mg g^{-1} in winter. The contents of TOC and TN decreased seaward from the river mouth to the shelf and increased southward along the narrow muddy area (Figures 2g–2j). The concentrations of NH_4^+ in the sediments were characterized by a significant seasonal variation (one-way ANOVA, $p < 0.001$),

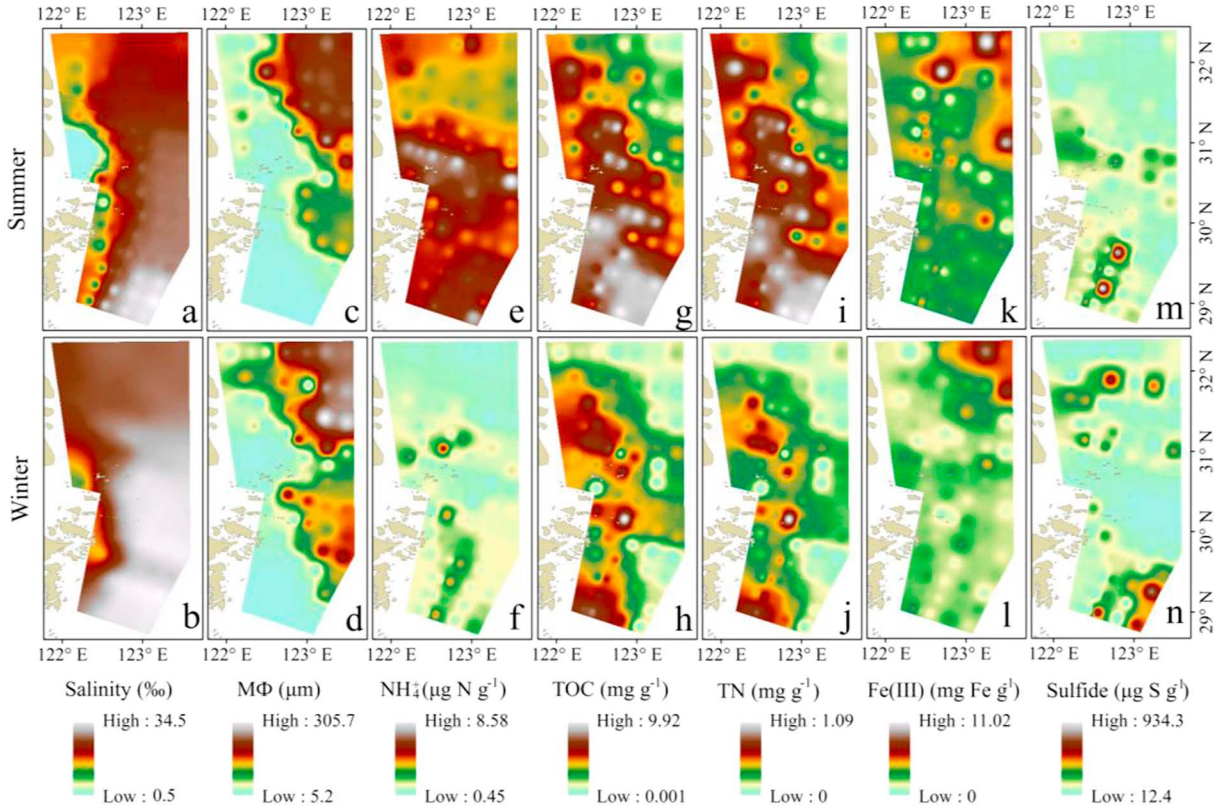

Figure 2. (a–n) Spatiotemporal distributions of physicochemical parameters in the sediments of the East China Sea (ECS). MΦ, NH_4^+, and Fe(III) denote median grain size, sediment NH_4^+, and sediment ferric oxides, respectively.

with values of 3.06–8.58 $\mu g\ N\ g^{-1}$ in summer and 0.45–5.35 $\mu g\ N\ g^{-1}$ in winter (Figures 2e and 2f and Table S1). The concentrations of Fe(III) varied from 0.64 to 11.02 $mg\ Fe\ g^{-1}$ in summer, with a mean value of $3.68 \pm 1.89\ mg\ Fe\ g^{-1}$, while they ranged from 0.26 to 8.95 $mg\ Fe\ g^{-1}$ in winter, with a mean value of $2.39 \pm 1.41\ mg\ Fe\ g^{-1}$. Also, Fe(III) was relatively enriched in the northeast of the study area, compared with other regions (Figures 2k and 2l). The concentrations of sulfide were in the range of 25.4–934.8 $\mu g\ S\ g^{-1}$ and 12.2–748.8 $\mu g\ S\ g^{-1}$ in summer and winter sediments, respectively, and sulfide hot spots occurred in the river mouth and south of the study area (Figures 2m and 2n).

3.2. Spatial and Temporal Variations of N Transformation Rates

GNM rates in summer varied from 0.11 to 6.10 $\mu g\ N\ g^{-1}\ d^{-1}$ with an average value of $2.52 \pm 1.56\ \mu g\ N\ g^{-1}\ d^{-1}$ (Figure 3a), while in winter, they ranged from 0.04 to 3.73 $\mu g\ N\ g^{-1}\ d^{-1}$ with an average of $1.26 \pm 1.04\ \mu g\ N\ g^{-1}\ d^{-1}$ (Figure 3b). The spatial distribution of GNM rates showed a similar pattern in both summer and winter. The annual mean GNM rates among these three regions (YEM, ZMCM, and SAN) were ranked as follows: ZMCM ($2.91 \pm 1.14\ \mu g\ N\ g^{-1}\ d^{-1}$) > YEM ($2.24 \pm 1.09\ \mu g\ N\ g^{-1}\ d^{-1}$) > SAN ($0.79 \pm 0.55\ \mu g\ N\ g^{-1}\ d^{-1}$), and a significant spatial difference in GNM rates was observed between the muddy area (ZMCM and YEM) and the sandy area (SAN) in both summer and winter ($p < 0.05$ for all comparisons; Table 1). Meanwhile, a decreasing trend of GNM rates was detected from the coast to offshore in the study area, and an increasing trend was found southward along the inner shelf of ECS, with a similar variation pattern to the TOC and TN contents and fine-grained sediments (Figures 3a and 3b). Additionally, a marked seasonal difference in GNM rates was found within these three regions (one-way ANOVA, $p = 0.005$ for ZMCM; $p < 0.0001$ for YEM and for SAN; Table 1). Overall, irrespective of seasons, relatively large GNM rates were observed mainly at sites located in the muddy area of the ECS.

Rates of GAI in the sediments ranged from 0.20 to 9.82 $\mu g\ N\ g^{-1}\ d^{-1}$ in summer and from undetectable to 4.73 $\mu g\ N\ g^{-1}\ d^{-1}$ in winter, with a significant seasonal variation throughout these three regions (one-way

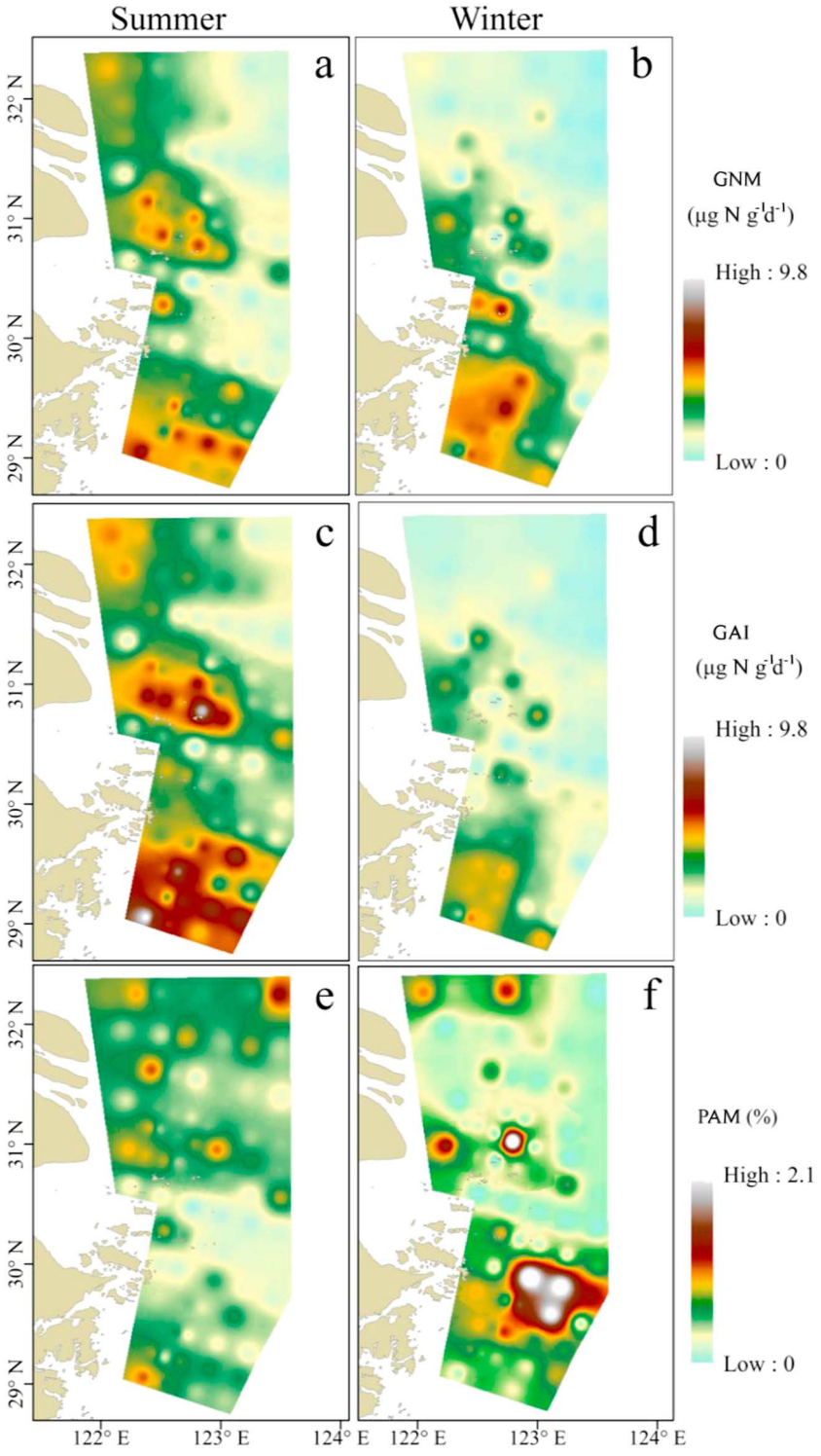

Figure 3. (a–f) Spatiotemporal variations of GNM and GAI rates, as well as PAM, in the sediments of the East China Sea (ECS).

ANOVA, $p < 0.0001$ for all correlations; Table 1). Spatially, GAI rates generally increased from the Yangtze Delta toward the southeast and decreased from the offshore to coast in both seasons. Also, there was a significant spatial variation in the annual mean rates among these three regions ($p < 0.05$; Table 1), and the mean values showed an order of ZMCM ($3.87 \pm 1.65\ \mu g\ N\ g^{-1}\ d^{-1}$) > YEM ($2.73 \pm 1.43\ \mu g\ N\ g^{-1}\ d^{-1}$) >

Table 1. Mean Values (±SD) of GNM, GAI, NO_3^-, NH_4^+, RAI, and PAM in the Sediments From the Yangtze Estuary Muddy Area (YEM), Zhe-Min Coastal Muddy Area (ZMCM), and Sandy Area (SAN)[a]

	YEM		ZMCM		SAN	
Items	Summer	Winter	Summer	Winter	Summer	Winter
GNM ($\mu g\ N\ g^{-1}\ d^{-1}$)	3.14 ± 1.35^{aA}	1.38 ± 0.85^{bB}	3.45 ± 1.42^{aA}	2.36 ± 0.85^{aB}	1.13 ± 0.68^{bA}	0.45 ± 0.42^{cB}
GAI ($\mu g\ N\ g^{-1}\ d^{-1}$)	3.76 ± 1.75^{bA}	1.69 ± 1.06^{bB}	4.91 ± 2.00^{aA}	2.83 ± 1.30^{aB}	1.64 ± 0.86^{cA}	0.66 ± 0.55^{cB}
RAI	1.23 ± 0.28^{aA}	1.32 ± 0.60^{abA}	1.51 ± 0.50^{bA}	1.19 ± 0.33^{aB}	1.57 ± 0.46^{bA}	1.57 ± 0.34^{aA}
PAM (%)	0.54 ± 0.28^{aA}	0.48 ± 0.59^{aA}	0.48 ± 0.23^{aA}	0.69 ± 0.51^{aB}	0.41 ± 0.26^{aA}	0.42 ± 0.64^{aA}
NH_4^+ ($\mu g\ N\ g^{-1}$)	5.36 ± 1.32^{aA}	1.63 ± 1.26^{bB}	5.42 ± 0.87^{aA}	1.91 ± 1.02^{aB}	4.34 ± 1.31^{bA}	1.25 ± 0.59^{cB}
NO_3^- ($\mu g\ N\ g^{-1}$)	0.76 ± 0.89^{aA}	0.89 ± 0.71^{aA}	0.62 ± 0.52^{aA}	0.81 ± 0.73^{aA}	0.32 ± 0.34^{bA}	0.43 ± 0.39^{bA}

[a]The significantly seasonal differences (at $p < 0.05$ according the F statistics) are marked by the different upper case letters. The significantly spatial differences (at $p < 0.05$ using Tukey's multiple comparison test) between YEM, ZMCM, and SAN are marked by the different lower case letters.

SAN ($1.15 \pm 0.71\ \mu g\ N\ g^{-1}\ d^{-1}$). In addition, there was a significant correlation between GAI and GNM rates in both seasons ($p < 0.01$; Figure 4).

In the study area, PAM (percentage of NH_4^+ mineralized per day) ranged between 0.03 and 1.25% in summer (Figure 3e) and between 0.01 and 2.89% in winter (Figure 3f). The mean PAM values among these three areas were in the following order of YEM ($0.54 \pm 0.28\%$) > ZMCM ($0.48 \pm 0.23\ \%$) > SAN ($0.41 \pm 0.26\%$) in summer and ZMCM ($0.69 \pm 0.5\%$) > YEM ($0.48 \pm 0.59\%$) > SAN ($0.43 \pm 0.64\%$) in winter (Table 1). Additionally, no significant seasonal variation in PAM was detected in the study area (excluding ZMCM; Table 1). In summer, the spatial distribution of PAM had several hot spots and declined generally from the north to south, while the winter PAM was generally higher in the muddy than sandy areas.

3.3. Environmental Parameters Affecting Rates

Irrespective of seasons, the relationships of environmental parameters with GNM and GAI rates are given in Table 2. In the ZMCM, GNM rates were positively correlated to sediment temperature, pH, NH_4^+, NO_3^-, TOC, TN, and clay contents but negatively correlated to sediment C:N ratio and sand content. GAI rates in the ZMCM exhibited the same relationships as GNM rates. In the YEM, temperature, pH, NH_4^+, NO_3^-, TOC, TN, and silt contents positively covaried with GNM rates, while bottom water salinity, sediment C:N ratio, and sand content exhibited a negative covariance with GNM rates. The relationships of GAI rates in the YEM with environmental parameters were similar to GNM rates. In the SAN, measured GNM and GAI rates were positively correlated with sediment temperature, pH, NO_3^-, TOC, TN, sulfide, and Fe(III) content but inversely correlated to sediment C:N ratio. When considering all sites, rates of GNM and GAI showed significant positive correlations with temperature, pH, clay content, NH_4^+, NO_3^-, TOC, and TN, while they were correlated negatively with sediment C:N ratio and sand content in the entire study area. In addition, comparison of the correlation matrices revealed that the significant correlation coefficients among rates and sulfide and Fe(III) content were observed in the SAN, but not in the muddy area (YEM and ZMCM) or the entire study area.

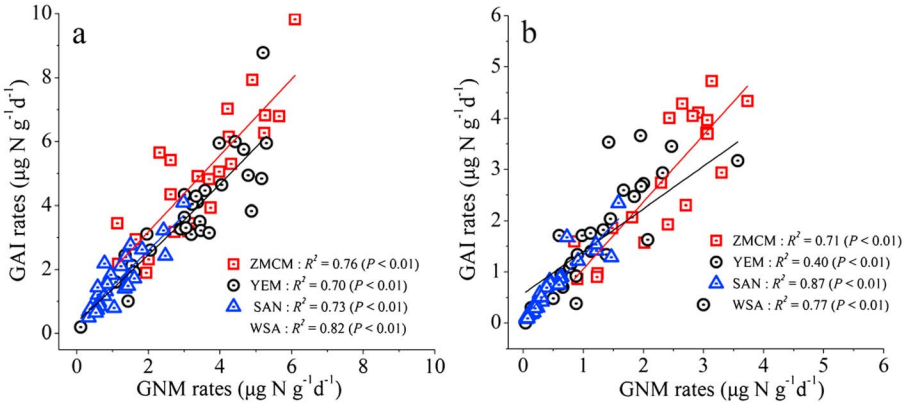

Figure 4. Pearson's correlations between GNM and GAI rates from the Yangtze Estuary muddy area (YEM), Zhe-Min Coastal muddy area (ZMCM), and sandy area (SAN), and whole study area (WSA) in (a) summer and (b) winter.

Table 2. Pearson's Correlations of Site Physico-chemical Parameters With GNM and GAI Rates for the Yangtze Estuary Muddy Area (YEM), Zhe-Min Coastal Muddy Area (ZMCM), and Sandy Area (SAN), and Whole Study Area (WSA)

	ZMCM ($n = 43$)		YEM ($n = 54$)		SAN ($n = 59$)		WSA ($n = 156$)	
Parameters	GNM	GAI	GNM	GAI	GNM	GAI	GNM	GAI
Depth	−0.08	−0.05	−0.16	−0.15	0.14	0.24	−0.14	−0.15
Temp	0.42**	0.53**	0.64**	0.61**	0.51**	0.57**	0.46**	0.49**
Salinity	−0.10	−0.11	−0.43**	−0.39**	−0.10	−0.01	−0.12	−0.14
pH	0.36*	0.44**	0.38**	0.26*	0.49**	0.52**	0.32**	0.31**
Clay	0.46**	0.48**	0.17	0.25	0.14	0.23	0.61**	0.63**
Silt	0.29	0.28	0.38**	0.37**	0.21	0.24	0.13	0.14
Sand	−0.36*	−0.32*	−0.35**	−0.36**	−0.03	−0.06	−0.63**	−0.60**
NH_4^+	0.43**	0.52**	0.59**	0.67**	0.60**	0.70**	0.58**	0.54**
NO_3^-	0.42**	0.35*	0.48**	0.43**	0.18	0.16	0.34**	0.39**
TOC	0.35*	0.43**	0.35**	0.36**	0.32*	0.34**	0.55**	0.57**
TN	0.33*	0.43**	0.31*	0.34**	0.38*	0.41**	0.55**	0.58**
C:N	−0.34*	−0.32*	−0.29*	−0.30**	−0.38**	-0.34*	−0.31**	−0.35**
Fe(III)	0.18	0.27	0.05	0.03	0.37**	0.47**	0.13	0.09
Sulfide	0.12	0.09	0.08	0.05	0.46**	0.35**	0.11	0.14

*Significant at $p < 0.05$.
**Significant at $p < 0.01$.

4. Discussion

In the present study, the spatial and seasonal changes in N mineralization and immobilization rates were investigated in the sediments of the ECS, which improves the understanding of N transformations in the coastal marine environment. Seasonally, both GNM and GAI rates in summer were significantly higher than those in winter (one-way ANOVA, $p < 0.0001$; Table 1). This seasonal pattern is likely due to the differences in temperature which was significantly higher in summer (21.05 ± 2.15°C) than in winter (9.57 ± 2.55°C) (one-way ANOVA, $p < 0.001$). Temperature is generally considered as an important factor regulating N mineralization and immobilization, because it can directly affect the physiological activity of microorganisms [*Grenon et al.*, 2004; *Von Lützow and Kögel-Knabner*, 2009]. It has been documented that GNM and GAI rates were significantly higher at high temperature (35°C) than at low temperature (15°C and 5°C), with fractional changes of 1.56–2.59 and 1.20–5.73 in rates with a 10°C increase in temperature (Q_{10}), respectively [*Lan et al.*, 2014]. Also, significantly positive correlations of both GNM and GAI rates with temperature were found throughout the study area ($p < 0.01$ for all correlations; Table 2). Hence, these relationships suggested the importance of temperature in controlling the seasonal changes of N mineralization and immobilization in the study area.

The spatial distribution showed that both GNM and GAI rates generally decreased from the inshore to offshore and from the north to south, and the higher rates were observed in the inshore region, especially in the Zhe-Min Coast (Figure 3). This distribution pattern was similar to the TOC and TN contents (Figures 3g–3j and and 5e and 5f), which is supported by the positive correlations of both GNM and GAI rates with sediment TOC and TN contents (Table 2). TOC has been considered to play a critical role in controlling N transformations, because it provides energy and materials for microbial metabolisms and thus affects sediment N mineralization and immobilization [*Kader et al.*, 2013]. Availability of TN supplies substrate for N mineralization, and N immobilization can subsequently be facilitated by the increasing accumulation of NH_4^+ derived from organic N decomposition [*Barrett and Burke*, 2000]. In addition, sediment C:N ratio negatively covaried with both GNM and GAI rates in the ECS (Table 2), indicating that TOC available contents and C:N stoichiometry might play an important role in sediment N mineralization and N immobilization in this ecosystem. A similar relationship between GNM rate and C:N ratio has been reported in other ecosystems [*Zhu et al.*, 2013b; *Regehr et al.*, 2015; *Zhao et al.*, 2015]. Hence, the spatial patterns of N mineralization and immobilization in the study area were remarkably affected by the bioavailability of TOC and TN.

The distribution of both GNM and GAI rates exhibited a similar pattern to fine-grained sediments, with relatively higher rates in the muddy than sandy areas (Figures 2 and 3). Meanwhile, N mineralization and immobilization rates were positively correlated with silt and clay contents, and negatively correlated with sediment

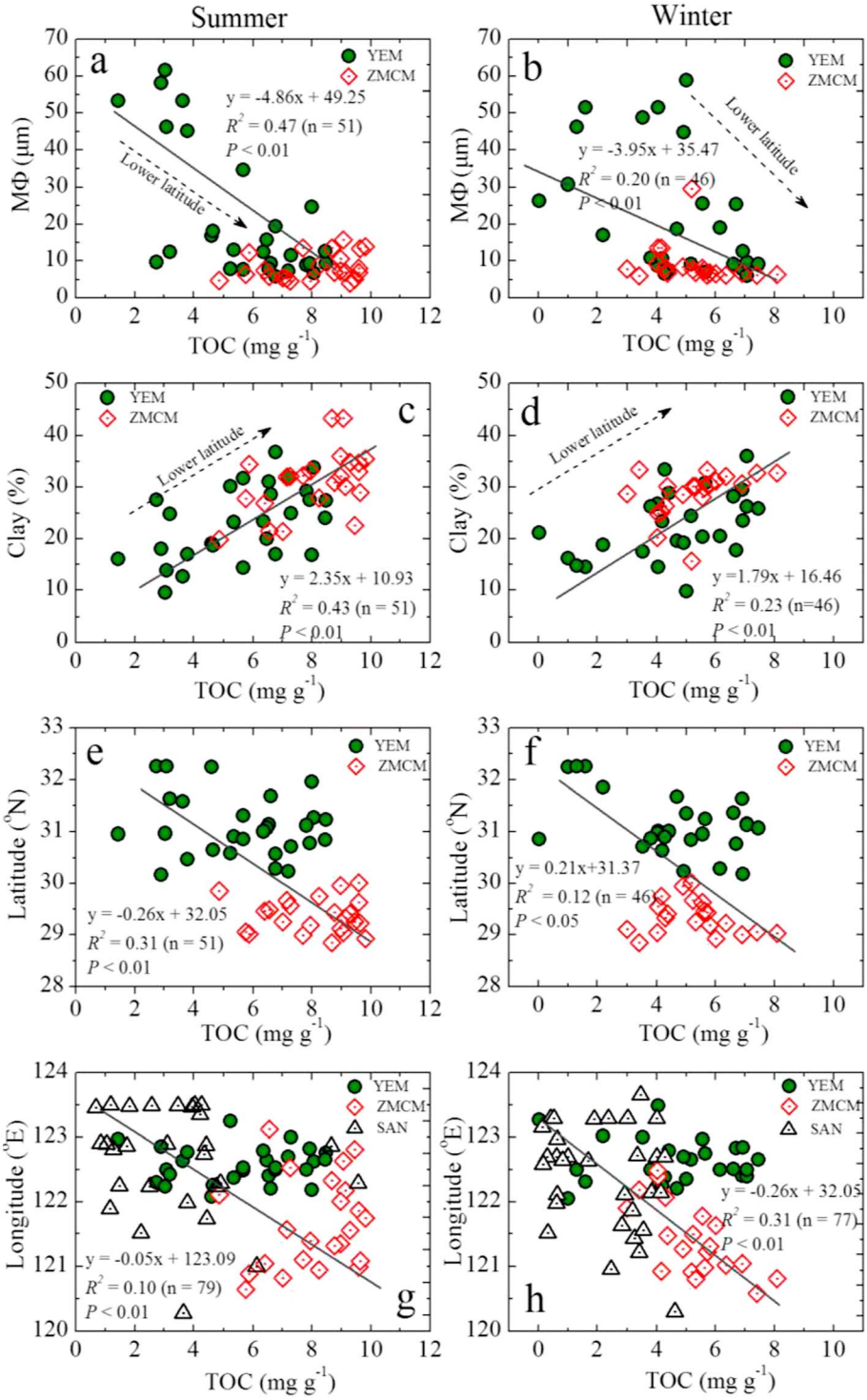

Figure 5. Pearson's correlations of TOC contents with sediment mean sizes (MΦ), clay contents, latitude and longitude in the East China Sea (ECS) for (a, c, e, and g) summer and (b, d, f, and h) winter.

MΦ and sand content (Table 2). Significant relationships of sediment MΦ with TOC and TN contents were also observed in this study ($p < 0.01$ in all correlations; Figure S1 in the supporting information). These relationships imply that fine-grained sediments are characterized by relatively high content of TOC and are more favorable to accumulate organic matter than coarse-grained sediments. In contrast, the coarse sediments

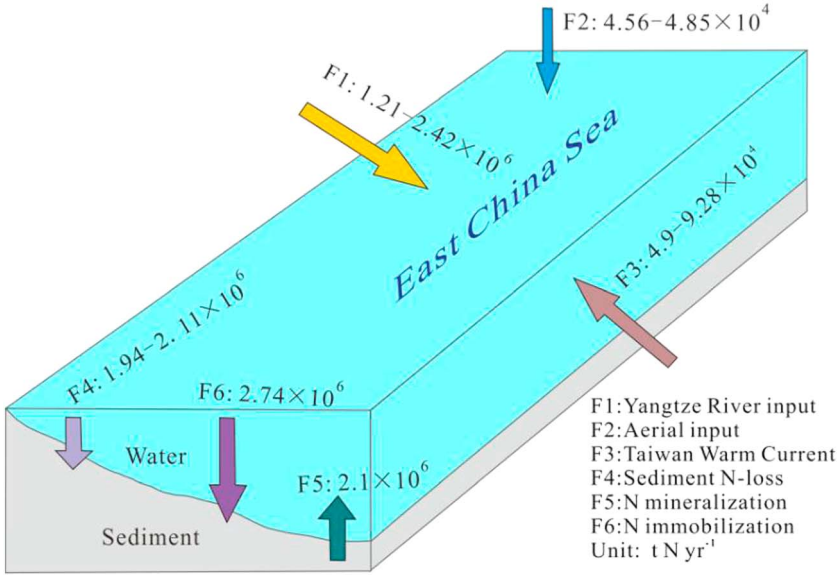

Figure 6. General fluxes of DIN in ECS; data on F1 from *Huang et al.* [2006], *Kim et al.* [2011], and *Xu et al.* [2013]; F2 from *Chen and Wang* [1999] and *Kim et al.* [2011]; F3 from *Chen and Wang* [1999]; F4 from *Liu et al.* [2010b] and *Su et al.* [2013]; F5 from *Song et al.* [2013], and unpublished data, which is calculated by denitrification plus anammox; and F6 and F7 from this study. The area assigned for calculation is 5.1×10^{10} m^2.

are characterized by high-density and generally composed of quartz and feldspar [*Yao et al.*, 2015]. Therefore, both GNM and GAI rates in the muddy sediments were significantly higher than those in the sandy sediments. A decreasing trend of both GNM and GAI rates was observed from the north to south in the muddy area (Figure 3). We also found that sediment TOC was positively correlated to clay content ($p < 0.01$ for both seasons; Figures 5c and 5d), but inversely correlated to sediment MΦ ($p < 0.01$ for both seasons; Figures 5a and 5b) and latitude ($p < 0.01$ for summer and $p < 0.05$ for winter; Figures 5e and 5f) in the muddy area. These results were likely because hydrodynamic sorting of riverine particles based on grain size and density has an important effect on the distribution of N mineralization and immobilization along the coastal margin. Due to the waves and tide-generated current forcing, sedimentary particulate matter may experience several cycles of deposition-resuspension-transport processes, and thus influence the quantity and type of sediments in the coastal and shelf ecosystem [*Zhu et al.*, 2011]. There are several intricate currents in the ECS (Figure 1b). Two southward currents (the Yellow Sea Coastal Current and the Zhe-Min Coastal Current) are generally more active in winter, which carry sediments and water from the Yangtze River southward along the inner shelf. However, in summer the Taiwan Warm Current is greatly intensified, which can weaken the southward transport of sediments along the Zhe-Min Coast. Therefore, fine-grained materials transported by the Yangtze River are likely to be first precipitated in the estuarine region during summer and then resuspended and remobilized southward during winter along the Zhe-Min Coast, consequently leading to the variation of surface sediment characteristics in space and time [*Wang et al.*, 2015; *Yao et al.*, 2015]. In addition, rates of GNM and GAI in the ZMCM were significant higher than those in the YEM in both seasons (except GNM rates in summer; Table 1). This difference in both rates between the ZMCM and YEM was not only related to TOC contents increasing from the YEM (mean: 5.64 ± 2.02 mg g^{-1} in summer and 4.65 ± 2.07 mg g^{-1} in winter) to the ZMCM (mean: 8.01 ± 1.64 mg g^{-1} in summer and 5.27 ± 1.37 mg g^{-1} in winter) but also connected to temperature that was higher in the ZMCM (mean: 22.97 ± 2.5°C in summer and 11.29 ± 1.82°C in winter) than in the YEM (mean: 19.63 ± 0.72°C in summer and 7.82 ± 1.86°C in winter). Overall, the spatiotemporal variation patterns of N transformations were not related directly to sediment grain size but indirectly influenced by available organic matter which in turn affected the N mineralization and immobilization.

It has been reported that pH, in the range of 4 to 8, can accelerate N mineralization with increasing pH [*Fu et al.*, 1987], mainly because pH alters microbial communities and abundance [*Högberg et al.*, 2007; *Rousk et al.*, 2009; *Cheng et al.*, 2013]. In this study, both GNM and GAI rates were also observed to correlate

positively with sediment pH (Table 2). However, the response of microbial dynamics to pH might not be an important mechanism resulting in the changes of GNM and GAI rates, because the range of pH (7.39–8.53) was relatively small in the ECS. Interestingly, pH was correlated positively to sediment temperature in the study area ($p < 0.01$). The autocorrelation between pH and sediment temperature might explain the observed relationships between pH and GNM/GAI rates. However, further work is still required to examine the effects of pH on N mineralization and immobilization. In addition, GNM rates were correlated significantly with NO_3^- contents in the sediments of the muddy area (YEM and ZMCM), while no significant relationship was observed in the sandy area (SAN; Table 2). This result was likely because sediment NO_3^- contents in the muddy area were significantly higher than those in the sandy area (Table 1) and NO_3^- as an electron donor can oxidize the organic material (equation (3)) [*Pena et al.*, 2010].

$$(CH2O)106(NH3)16H3PO4 + 84.8HNO3 \rightarrow 106CO2 + 42.4N2 + 148.4H2O + 16NH3 + H3PO4 \quad (3)$$

In contrast, N mineralization rates in the sandy area were positively correlated to sulfide and Fe(III) concentrations (Table 2). These relationships were likely attributed to relatively high availability of Fe(III) and sulfate as electron acceptors for N mineralization in the NO_3^--limited region (equations (4) and (5)) [*Risgaard-Petersen et al.*, 2012].

$$(CH2O)106(NH3)16H3PO4 + 424FeOOH + 848H^+ \rightarrow 106CO2 + 742H2O + 424Fe^{2+} + 16NH3 + H3PO4 \quad (4)$$

$$(CH2O)106(NH3)16H3PO4 + 53SO_4^{2-} + 106H^+ \rightarrow 106CO2 + 106H2O + 53H2S + 16NH3 + H3PO4 \quad (5)$$

Therefore, these results imply that the pathways of sediment N mineralization are significantly affected by the distributions of available electron acceptors in the study area [*Santschi et al.*, 1990].

GNM rates measured in this study were comparable to the rates reported in grassland [*Corre et al.*, 2002; *Accoe et al.*, 2004; *Cheng et al.*, 2012], and other estuarine and marine ecosystems [*Blackburn*, 1979; *Cufrey and Kemp*, 1992; *Lin et al.*, 2016], but lower than those reported in wetland [*Bedard-Haughn et al.*, 2006; *Jin et al.*, 2012], agricultural [*Luxhøi et al.*, 2006], and forest [*Cheng et al.*, 2012; *Zhu et al.*, 2013b] ecosystems (Table S2). In addition, the measured rates of GNM were much higher than the net N mineralization rates from other estuarine and coastal marine ecosystems (Table S2) [*Billen*, 1978; *Boynton et al.*, 1980; *Jensen et al.*, 1990; *Rysgaard et al.*, 2000], probably showing high N regeneration rates in the study area. Meanwhile, GAI rates determined in this study were comparable with those from other ecosystems (Table S2) [*Corre et al.*, 2002; *Accoe et al.*, 2004; *Luxhøi et al.*, 2006; *Jin et al.*, 2012; *Cheng et al.*, 2012; *Zhu et al.*, 2013b]. We also found that both GNM and GAI rates were strongly interrelated throughout the study area ($p < 0.05$; Figure 4), which was consistent with the findings of previous studies [*Corre et al.*, 2002; *Bengtsson et al.*, 2003; *Zhu et al.*, 2013b] for wetland, grassland, forest, and agriculture ecosystems. This tight correlation between GNM and GAI rates indicated that NH_4^+ immobilization can be facilitated by the availability of readily mineralizable organic substrate. It might be expected that the factors controlling NH_4^+ assimilation would be similar to those affecting N mineralization, probably because the sediment microflora is responsible for both release and uptake of NH_4^+ [*Booth et al.*, 2005]. In addition, it should be noted that GAI rates might be overestimated in the ^{15}N-isotope dilution experiments because the substrates ($^{15}NH_4^+$) added to the sediments probably stimulated microbial mechanisms, and thus, they were probably lower under in situ conditions [*Davidson et al.*, 1991]. Accordingly, our estimated rates might not represent the rates of GAI that took place in the field but rather reflect the potential activity in the sediments of the ECS.

Sediment N mineralization and immobilization play a significant role in the N cycle in coastal marine ecosystems. Although these processes are critical for understanding of the N budget and maintenance of the ecological and environmental health in coastal marine ecosystems, few studies have examined sediment N mineralization and immobilization in the ESC. Thus, based on the potential rates of N mineralization and immobilization, the annual mineralized N and immobilized N (F) in the sediments of the ECS were estimated according to the following equation:

$$F = \frac{1}{2}\left(\sum_{i=1}^{78} mi \cdot di + \sum_{j=1}^{78} mj \cdot dj\right) \cdot a \cdot s \cdot h \cdot t \quad (6)$$

where F ($t\,N\,yr^{-1}$) denotes the annual mineralized N or immobilized N in the study area; m_i and m_j ($\mu g\,N\,g^{-1}\,d^{-1}$) denote the rates of GNM or GAI in the summer and winter sediment samples, respectively; d_i and d_j ($g\,cm^{-3}$) denote the dry density of summer and winter sediments, respectively (Table S1); a denotes

the unit conversion factor, which is equivalent to 1×10^{-8}; s (m^2) denotes the area of this study (approximately 5.1×10^{10} m^2), which was calculated with ArcGIS10.2 software; h (cm) denotes the sampling depth (5 cm); t denotes the time (365 days). The total mineralized and immobilized N were estimated at approximately 2.1×10^6 t N yr^{-1} and 2.7×10^6 t N yr^{-1}, respectively. In order to further assess the potential contributions of N mineralization and immobilization to the N budget, they were compared with other dissolved inorganic N (DIN) inputs and outputs in this study area (Figure 6). The total mineralized N was considerably similar to the riverine flux ($1.2–2.42 \times 10^6$ t N yr^{-1}) [*Huang et al.*, 2006; *Kim et al.*, 2011; *Xu et al.*, 2013], and much higher than the inputs from the Taiwan Warm Current ($4.90–9.28 \times 10^4$ t N yr^{-1}) [*Chen and Wang*, 1999] and the atmosphere ($4.56–4.85 \times 10^4$ t N yr^{-1}) [*Chen and Wang*, 1999; *Kim et al.*, 2011]. These comparisons indicated that the mineralization of sediment N is an important internal source of DIN and may partly contribute to exacerbation of coastal eutrophication and harmful algal blooms. In general, the ratio of GAI to GNM rates (RAI) ≥ 1 indicates an N-limited environment, whereas the RAI value of ≈0.5 indicates N saturation [*Aber*, 1992]. In this study, the values of RAI were ≥1 at most of sampling sites (Table 1 and Figure S2). Thus, the DIN from the sediment N mineralization may be a crucial contributor to the nutrient supply for phytoplankton growth in this N-limited ecosystem. Also, the amount of sediment N immobilization (2.7×10^6 t N yr^{-1}) estimated in this study was higher than the N-loss through both denitrification and anammox ($1.94–2.11 \times 10^6$ t N yr^{-1}) in the sediments of the ECS [*Song et al.*, 2013, and unpublished data], showing that sediment N immobilization may play an important role in maintaining the ecological and environmental health in this aquatic ecosystem.

5. Conclusions

This study investigated N mineralization and immobilization in the sediments of the ECS, with ^{15}N isotope dilution technique. The measured rates of GNM and GAI in the study area ranged from 0.04 to 6.1 μg N g^{-1} d^{-1} and from undetectable to 9.82 μg N g^{-1} d^{-1}, respectively. The rates of both GNM and GAI were greater in summer than in winter, and relative high rates were detected in the muddy area of the ECS. Nitrogen mineralization and immobilization were related closely to sediment temperature, pH, NH_4^+, NO_3^-, TOC, and TN contents in the muddy area, while they were dependent strongly on sediment temperature, pH, NH_4^+, TOC, TN, sulfide, and Fe (III) concentrations in the sandy area. Additionally, the total mineralized and immobilized N in the ECS were estimated to be approximately 2.1×10^6 t N yr^{-1} and 2.7×10^6 t N yr^{-1}, respectively. Compared with other inputs of DIN in this study area, the potential mineralized N could be an important internal DIN source, while the potential immobilized N could be an important DIN sink. Overall, this study shows the environmental significance of these processes in controlling the N budget of the coastal marine ecosystem.

Acknowledgments

This work was supported by the Chinese National Key Programs for Fundamental Research and Development (2016YFA0600904) and the Natural Science Foundations of China (41130525, 41322002, 41671463, and 41271114). Thanks are given to Wayne S. Gardner and anonymous reviewers for their constructive comments on the manuscript. Data presented in this paper can be obtained by sending a written request to the corresponding authors.

References

Aber, J. D. (1992), Nitrogen cycling and nitrogen saturation in temperate forest ecosystems, *Trends Ecol. Evol.*, *7*(7), 220–224.

Accoe, F., P. Boeckx, J. Busschaert, G. Hofman, and O. Van Cleemput (2004), Gross N transformation rates and net N mineralisation rates related to the C and N contents of soil organic matter fractions in grassland soils of different age, *Soil Biol. Biochem.*, *36*(12), 2075–2087.

Anderson, I. C., C. R. Tobias, B. B. Neikirk, and R. L. Wetzel (1997), Development of a process-based nitrogen mass balance model for a Virginia (USA) *Spartina alterniflora* salt marsh: Implications for net DIN flux, *Mar. Ecol. Prog. Ser.*, *159*, 13–27.

Barrett, J. E., and I. C. Burke (2000), Potential nitrogen immobilization in grassland soils across a soil organic matter gradient, *Soil Biol. Biochem.*, *32*(11), 1707–1716.

Bedard-Haughn, A., A. L. Matson, and D. J. Pennock (2006), Land use effects on gross nitrogen mineralization, nitrification, and N_2O emissions in ephemeral wetlands, *Soil Biol. Biochem.*, *38*(12), 3398–3406.

Bedard-Haughn, A., L. P. Comeau, and A. Sangster (2013), Gross nitrogen mineralization in pulse-crop rotations on the Northern Great Plains, *Nutr. Cycling Agroecosyst.*, *95*(2), 159–174.

Benbi, D. K., and J. Richter (2002), A critical review of some approaches to modelling nitrogen mineralization, *Biol. Fertil. Soils*, *35*(3), 168–183.

Bengtsson, G., P. Bengtson, and K. F. Månsson (2003), Gross nitrogen mineralization, immobilization, and nitrification rates as a function of soil C/N ratio and microbial activity, *Soil Biol. Biochem.*, *35*(1), 143–154.

Billen, G. (1978), A budget of nitrogen recycling in North Sea sediments off the Belgian coast, *Estuarine Coastal Mar. Sci.*, *7*(2), 127–146.

Blackburn, T. H. (1979), Method for measuring rates of NH_4^+ turnover in anoxic marine sediments, using a ^{15}N-NH_4^+ dilution technique, *Appl. Environ. Microb.*, *37*(4), 760–765.

Booth, M. S., J. M. Stark, and E. Rastetter (2005), Controls on nitrogen cycling in terrestrial ecosystems: A synthetic analysis of literature data, *Ecol. Monogr.*, *75*(2), 139–157.

Boynton, W. R., W. M. Kemp, and C. G. Osborne (1980), Nutrient fluxes across the sediment-water interface in the turbid zone of a coastal plain estuary, in *Estuarine Perspectives*, edited by W. S. Kennedy, pp. 93–109 , Academic Press, New York.

Caraco, N. F., G. Lampman, J. J. Cole, K. E. Limburg, M. L. Pace, and D. Fischer (1998), Microbial assimilation of DIN in a nitrogen rich estuary: Implications for food quality and isotope studies, *Mar. Ecol. Prog. Ser.*, *167*, 59–71.

Chen, C. T. A., and S. L. Wang (1999), Carbon, alkalinity and nutrient budgets on the East China Sea continental shelf, *J. Geophys. Res.*, *104*, 20,675–20,686, doi:10.1029/1999JC900055.

Chen, F., L. J. Hou, M. Liu, Y. L. Zheng, G. Y. Yin, X. B. Lin, X. F. Li, H. B. Zong, F. Y. Deng, and J. Gao (2016), Net anthropogenic nitrogen inputs (NANI) into the Yangtze River basin and the relationship with riverine nitrogen export, *J. Geophys. Res. Biogeosci.*, *121*, 451–465, doi:10.1002/2015JG003186.

Cheng, Y., Z. C. Cai, J. B. Zhang, M. Lang, B. Mary, and S. X. Chang (2012), Soil moisture effects on gross nitrification differ between adjacent grassland and forested soils in central Alberta, Canada, *Plant Soil*, *352*(1–2), 289–301.

Cheng, Y., J. Wang, B. Mary, J. B. Zhang, Z. C. Cai, and S. X. Chang (2013), Soil pH has contrasting effects on gross and net nitrogen mineralizations in adjacent forest and grassland soils in central Alberta, Canada, *Soil Biol. Biochem.*, *57*, 848–857.

Corre, M. D., R. R. Schnabel, and W. L. Stout (2002), Spatial and seasonal variation of gross nitrogen transformations and microbial biomass in a Northeastern US grassland, *Soil Biol. Biochem.*, *34*(4), 445–457.

Cufrey, J. M., and W. M. Kemp (1992), Influence of the submersed plant, Potamogeton perfoliatus, on nitrogen cycling in estuarine sediments, *Limnol. Oceanogr.*, *37*(7), 1483–1495.

Cui, S. H., Y. L. Shi, P. M. Groffman, W. H. Schlesinger, and Y. G. Zhu (2013), Centennial-scale analysis of the creation and fate of reactive nitrogen in China (1910–2010), *Proc. Natl. Acad. Sci. U.S.A.*, *110*(6), 2052–2057.

Davidson, E. A., S. C. Hart, C. A. Shanks, and M. K. Firestone (1991), Measuring gross nitrogen mineralization, and nitrification by ^{15}N isotopic pool dilution in intact soil cores, *J. Soil Sediment*, *42*(3), 335–349.

Deng, F. Y., L. J. Hou, M. Liu, Y. L. Zheng, G. Y. Yin, X. F. Li, X. B. Lin, F. Chen, J. Gao, and X. F. Jiang (2015), Dissimilatory nitrate reduction processes and associated contribution to nitrogen removal in sediments of the Yangtze Estuary, *J. Geophys. Res. Biogeosci.*, *120*, 1521–1531, doi:10.1002/2015JG003007.

Di, H., K. Cameron, and R. McLaren (2000), Isotopic dilution methods to determine the gross transformation rates of nitrogen, phosphorus, and sulfur in soil: A review of the theory, methodologies, and limitations, *Soil Res.*, *38*(1), 213–230.

Fu, M. H., X. C. Xu, and M. A. Tabatabai (1987), Effect of pH on nitrogen mineralization in crop-residue-treated soils, *Biol. Fertil. Soils*, *5*(2), 115–119.

Gao, L., D. J. Li, and Y. W. Zhang (2012), Nutrients and particulate organic matter discharged by the Changjiang (Yangtze River): Seasonal variations and temporal trends, *J. Geophys. Res.*, *117*, G4001, doi:10.1029/2012JG001952.

Gao, L., D. J. Li, J. J. Ishizaka, Y. W. Zhang, H. B. Zong, and L. D. Guo (2015), Nutrient dynamics across the river-sea interface in the Changjiang (Yangtze River) estuary-East China Sea region, *Limnol. Oceanogr.*, *60*(6), 2207–2221.

Grenon, F., R. L. Bradley, and B. D. Titus (2004), Temperature sensitivity of mineral N transformation rates, and heterotrophic nitrification: Possible factors controlling the post-disturbance mineral N flush in forest floors, *Soil Biol. Biochem.*, *36*(9), 1465–1474.

Gütlein, A., M. Dannenmann, and R. Kiese (2016), Gross nitrogen turnover rates of a tropical lower montane forest soil: Impacts of sample preparation and storage, *Soil Biol. Biochem.*, *95*, 8–10.

Hansen, L. S., and T. H. Blackburn (1991), Aerobic and anaerobic mineralization of organic material in marine sediment microcosms, *Mar. Ecol. Prog. Ser.*, *75*, 283–291.

Herbert, R. (1999), Nitrogen cycling in coastal marine ecosystems, *FEMS Microbiol. Rev.*, *23*(5), 563–590.

Högberg, M. N., Y. Chen, and P. Högberg (2007), Gross nitrogen mineralisation and fungi-to-bacteria ratios are negatively correlated in boreal forests, *Biol. Fertil. Soils*, *44*(2), 363–366.

Hou, L. J., Y. L. Zheng, M. Liu, J. Gong, X. L. Zhang, G. Y. Yin, and L. You (2013), Anaerobic ammonium oxidation (anammox) bacterial diversity, abundance, and activity in marsh sediments of the Yangtze Estuary, *J. Geophys. Res. Biogeosci.*, *118*, 1237–1246, doi:10.1002/jgrg.20108.

Huang, Q. H., H. T. Shen, Z. J. Wang, X. C. Liu, and R. B. Fu (2006), Influences of natural and anthropogenic processes on the nitrogen and phosphorus fluxes of the Yangtze Estuary, China, *Reg. Environ. Change*, *6*(3), 125–131.

Huygens, D., M. Trimmer, T. Rütting, C. Müller, C. M. Heppell, K. Lansdown, and P. Boeckx (2013), Biogeochemical nitrogen cycling in wetland ecosystems: Nitrogen-15 isotope techniques, in *Methods in Biogeochemistry of Wetlands*, edited by R. D. DeLaune et al., pp. 553–592 , Soil Sci. Soc. AM, Madison, Wisconsin.

Jensen, M. H., E. Lomstein, and J. Sørensen (1990), Benthic NH_4^+ and NO_3^- flux following sedimentation of a spring phytoplankton bloom in Aarhus Bight, Denmark, *Mar. Ecol. Prog. Ser.*, *61*, 87–96.

Jin, X. B., J. Y. Huang, and Y. K. Zhou (2012), Impact of coastal wetland cultivation on microbial biomass, ammonia-oxidizing bacteria, gross N transformation and N_2O and NO potential production, *Biol. Fertil. Soils*, *48*(4), 363–369.

Kader, M., S. Sleutel, S. A. Begum, and A. Z. M. Moslehuddin (2013), Nitrogen mineralization in sub-tropical paddy soils in relation to soil mineralogy, management, pH, carbon, nitrogen and iron contents, *Eur. J. Soil Sci.*, *64*(1), 47–57.

Kalvelage, T., G. Lavik, P. Lam, S. Contreras, L. Arteaga, C. R. Löscher, A. Oschlies, A. Paulmier, L. Stramma, and M. M. Kuypers (2013), Nitrogen cycling driven by organic matter export in the South Pacific oxygen minimum zone, *Nat. Geosci.*, *6*(3), 228–234.

Kim, T. W., K. Lee, R. G. Najjar, H. D. Jeong, and H. J. Jeong (2011), Increasing N abundance in the northwestern Pacific Ocean due to atmospheric nitrogen deposition, *Science*, *334*(6055), 505–509.

Kirkham, D. O. N., and W. V. Bartholomew (1954), Equations for following nutrient transformations in soil, utilizing tracer data, *Soil Sci. Soc. Am. J.*, *18*(1), 33–34.

Lan, T., Y. Han, M. Roelcke, R. Nieder, and Z. C. Cai (2014), Temperature dependence of gross N transformation rates in two Chinese paddy soils under aerobic condition, *Biol. Fertil. Soils*, *50*(6), 949–959.

Li, X. A., Z. M. Yu, X. X. Song, X. H. Cao, and Y. Q. Yuan (2011), Nitrogen and phosphorus budgets of the Changjiang River estuary, *Chin. J. Oceanol. Limn.*, *29*(4), 762–774.

Li, X. F., L. J. Hou, M. Liu, X. B. Lin, Y. Li, and S. W. Li (2014), Primary effects of extracellular enzyme activity and microbial community on carbon and nitrogen mineralization in estuarine and tidal wetlands, *Appl. Microbiol. Biot.*, *99*(6), 1–15.

Lin, X. B., L. J. Hou, M. Liu, X. F. Li, G. Y. Yin, Y. L. Zheng, and F. Y. Deng (2016), Gross nitrogen mineralization in surface sediments of the Yangtze Estuary, *PLoS One*, *11*(3, e0151930).

Liu, H., Q. He, Z. B. Wang, G. J. Weltje, and J. Zhang (2010a), Dynamics and spatial variability of near-bottom sediment exchange in the Yangtze Estuary, China, *Estuarine Coastal Mar. Sci* , *86*(3), 322–330.

Liu, J. P., K. H. Xu, A. C. Li, J. D. Milliman, D. M. Velozzi, S. B. Xiao, and Z. S. Yang (2007), Flux and fate of Yangtze River sediment delivered to the East China Sea, *Geomorphology*, *85*(3), 208–224.

Liu, K. K., S. Y. Chao, H. J. Lee, G. C. Gong, and Y. C. Teng (2010b), Seasonal variation of primary productivity in the East China Sea: A numerical study based on coupled physical-biogeochemical model, *Deep Sea Res., Part II*, *57*(19), 1762–1782.

Luxhøi, J., S. Bruun, B. Stenberg, T. A. Breland, and L. S. Jensen (2006), Prediction of gross and net nitrogen mineralization-immobilization-turnover from respiration, *Soil Sci. Soc. Am. J.*, *70*(4), 1121–1128.

Matheson, F. E., M. L. Nguyen, A. B. Cooper, and T. P. Burt (2003), Short-term nitrogen transformation rates in riparian wetland soil determined with nitrogen-15, *Biol. Fertils. Soils*, *38*(3), 129–136.

Mishra, S., H. J. Di, K. C. Cameron, R. Monaghan, and A. Carran (2005), Gross nitrogen mineralisation rates in pastural soils and their relationships with organic nitrogen fractions, microbial biomass and protease activity under glasshouse conditions, *Biol. Fertils. Soils*, *42*(1), 45–53.

Ni, J. Y., X. Y. Liu, Q. J. Chen, and Y. Lin (2006), Pore-water distribution and quantification of diffusive benthic fluxes of nutrients in the Huanghai and East China Seas sediments, *Acta Oceanol. Sin.*, *25*(1), 90–99.

Pena, M., S. Katsev, T. Oguz, and D. Gilbert (2010), Modeling dissolved oxygen dynamics and hypoxia, *Biogeosciences*, *7*(3), 933–957.

Qin, Y. (1996), *Geology of the East China Sea*, Science Press, Beijing.

Regehr, A., M. Oelbermann, C. Videla, and L. Echarte (2015), Gross nitrogen mineralization and immobilization in temperate maize-soybean intercrops, *Plant Soil*, *391*, 353–365.

Risgaard-Petersen, N., A. Revil, P. Meister, and L. P. Nielsen (2012), Sulfur, iron-, and calcium cycling associated with natural electric currents running through marine sediment, *Geochim. Cosmochim. Acta*, *92*, 1–13.

Roden, E. E., and D. R. Lovley (1993), Evaluation of ^{55}Fe as a tracer of Fe(III) reduction in aquatic sediments, *Geomicrobiol. J.*, *11*(1), 49–56.

Rousk, J., P. C. Brookes, and E. Bååth (2009), Contrasting soil pH effects on fungal and bacterial growth suggest functional redundancy in carbon mineralization, *Appl. Environ. Microbiol.*, *75*(6), 1589–1596.

Rysgaard, S., P. B. Christensen, M. V. Sørensen, P. Funch, and P. Berg (2000), Marine meiofauna, carbon and nitrogen mineralization in sandy and soft sediments of Disko Bay, West Greenland, *Aquat. Microbiol. Ecol.*, *21*(1), 59–71.

Santschi, P., P. Höhener, G. Benoit, and M. B. Brink (1990), Chemical process at the sediment-water interface, *Mar. Chem.*, *30*, 269–315.

Song, G. D., S. M. Liu, H. Marchant, M. M. M. Kuypers, and G. Lavik (2013), Anammox, denitrification and dissimilatory nitrate reduction to ammonium in the East China Sea sediment, *Biogeosciences*, *10*(11), 6851–6864.

Su, N., J. Z. Du, Y. Li, and J. Zhang (2013), Evaluation of surface water mixing and associated nutrient fluxes in the East China Sea using ^{226}Ra and ^{228}Ra, *Mar. Chem.*, *156*, 108–119.

Tremblay, L., and R. Benner (2006), Microbial contributions to N-immobilization and organic matter preservation in decaying plant detritus, *Geochim. Cosmochim. Acta*, *70*(1), 133–146.

Von Lützow, M., and I. Kögel-Knabner (2009), Temperature sensitivity of soil organic matter decomposition-what do we know?, *Biol. Fertil. Soils*, *46*(1), 1–15.

Wang, J. L., J. Z. Du, M. Baskaran, and J. Zhang (2016), Mobile mud dynamics in the East China Sea elucidated using ^{210}Pb, ^{137}Cs, ^{7}Be, and ^{234}Th as tracers, *J. Geophys. Res. Oceans*, *121*, 224–239, doi:10.1002/2015JC011300.

Wang, J. P., P. Yao, T. S. Bianchi, D. Li, B. Zhao, X. Q. Cui, H. H. Pan, T. T. Zhang, and Z. G. Yu (2015), The effect of particle density on the sources, distribution, and degradation of sedimentary organic carbon in the Changjiang Estuary and adjacent shelf, *Chem. Geol.*, *402*, 52–67.

Wu, P., R. Bi, S. S. Duan, H. Jin, J. F. Chen, Q. Hao, Y. M. Cai, X. Y. Mao, and M. X. Zhao (2016), Spatiotemporal variations of phytoplankton in the East China Sea and the Yellow Sea revealed by lipid biomarkers, *J. Geophys. Res. Biogeosci.*, *121*, 109–125, doi:10.1002/2015JG003167.

Xu, H., E. Wolanski, and Z. Y. Chen (2013), Suspended particulate matter affects the nutrient budget of turbid estuaries: Modification of the LOICZ model and application to the Yangtze Estuary, *Estuarine Coastal Mar. Sci*, *127*, 59–62.

Yao, P., Z. G. Yu, T. S. Bianchi, Z. G. Guo, M. X. Zhao, C. S. Knappy, B. J. Keely, B. Zhao, T. T. Zhang, and H. H. Pan (2015), A multiproxy analysis of sedimentary organic carbon in the Changjiang Estuary and adjacent shelf, *J. Geophys. Res. Biogeosci.*, *120*, 1407–1429, doi:10.1002/2014JG002831.

Yin, G. Y., L. J. Hou, M. Liu, Z. F. Liu, and W. S. Gardner (2014), A novel membrane inlet mass spectrometer method to measure $^{15}NH_4^+$ for isotope-enrichment experiments in aquatic ecosystems, *Environ. Sci. Technol.*, *48*(16), 9555–9562.

Yu, Y., J. M. Song, X. G. Li, and L. Q. Duan (2012), Geochemical records of decadal variations in terrestrial input and recent anthropogenic eutrophication in the Changjiang Estuary and its adjacent waters, *Appl. Geochem.*, *27*(8), 1556–1566.

Zhang, A. Y., J. Zhang, J. Hu, R. F. Zhang, and G. S. Zhang (2015), Silicon isotopic chemistry in the Changjiang Estuary and coastal regions: Impacts of physical and biogeochemical processes on the transport of riverine dissolved silica, *J. Geophys. Res. Oceans*, *120*, 6943–6957, doi:10.1002/2015JC011050.

Zhang, G. L., J. Zhang, Y. B. Kang, and S. M. Liu (2004), Distributions and fluxes of methane in the East China Sea and the Yellow Sea in spring, *J. Geophys. Res.*, *109*, C07011, doi:10.1029/2004JC002268.

Zhao, W., Z. C. Cai, and Z. H. Xu (2015), Net and gross N transformation rates in subtropical forest soils under aerobic and anaerobic conditions, *J. Soil Sediment*, *15*(1), 96–105.

Zheng, Y. L., L. J. Hou, S. Newell, M. Liu, J. L. Zhou, H. Zhao, L. L. You, and X. L. Cheng (2014), Community dynamics and activity of ammonia-oxidizing prokaryotes in intertidal sediments of the Yangtze Estuary, *Appl. Environ. Microbiol.*, *80*(1), 408–419.

Zheng, Y., et al. (2016), Tidal pumping facilitates dissimilatory nitrate reduction in intertidal marshes, *Sci. Rep.*, *6*, 21338, doi:10.1038/srep21338.

Zhu, C., Z. H. Wang, B. Xue, P. S. Yu, J. M. Pan, T. Wagner, and R. D. Pancost (2011), Characterizing the depositional settings for sedimentary organic matter distributions in the Lower Yangtze River-East China Sea Shelf System, *Estuarine Coastal Mar. Sci*, *93*(3), 182–191.

Zhu, L., Y. Chen, L. Guo, and F. J. Wang (2013a), Estimate of dry deposition fluxes of nutrients over the East China Sea: The implication of aerosol ammonium to non-sea-salt sulfate ratio to nutrient deposition of coastal oceans, *Atmos. Environ.*, *69*, 131–138.

Zhu, T. B., T. Z. Meng, J. B. Zhang, Y. F. Yin, Z. C. Cai, W. Y. Yang, and W. H. Zhong (2013b), Nitrogen mineralization, immobilization turnover, heterotrophic nitrification, and microbial groups in acid forest soils of subtropical China, *Biol. Fertils. Soils*, *49*(3), 323–331.